Parabrachial *Calca* neurons mediate second-order conditioning

Sekun Park[1,2], Anqi Zhu[1,2], Feng Cao[1,2] and Richard Palmiter[1,2,3]

1. Department of Biochemistry, University of Washington, Seattle WA 98195 USA
2. Howard Hugues Medical Institute, University of Washington, Seattle WA 98195 USA
3. Department of Genome Science, University of Washington, Seattle WA 98195 USA

Abstract

Learning to associate cues, both directly and indirectly, with biologically significant events is essential for survival. Second-order conditioning (SOC) involves forming an association between a previously reinforced conditioned stimulus (CS1) and a new conditioned stimulus (CS2) without the presence of an unconditioned stimulus (US). The neural substrates mediating SOC, however, remain unclear. In the parabrachial nucleus, *Calca* gene-expressing neurons, which react to the noxious US, also respond to a CS after its pairing with a US. This observation led us to hypothesize their involvement in SOC. To explore this possibility, we established an aversive SOC behavioral paradigm in mice and monitored *Calca* neuron activity via single-cell calcium imaging during SOC and subsequent recall phases. These neurons were activated not only by CS1 following its association with the US but also by CS2 after SOC. Chemogenetically inhibiting these neurons during second-order associations attenuated SOC. These findings suggest that activating the US pathway in response to a learned CS plays an important role in forming the association between the old and a new CS, promoting the formation of second-order memories. (180 words)

Introduction

Remembering salient stimuli in the surrounding environment is crucial for predicting potential benefit or danger, impacting an animal's survival. Pavlovian conditioning has been extensively studied to understand underlying neural substrates and learning mechanisms[1–8]. It has been widely accepted because of the simplicity of CS and US, rapid learning, robust conditioned responses, and universality across species[9]. The dynamic and complex nature of environments rewards animals that use all available information for more precise prediction[10,11]. Responding to the earliest cue that predicts an outcome is an advantageous strategy and resembles the higher-order learning commonly observed in pets when learning to respond to cues that predict the availability of treats.

While Pavlov is credited with rigorous description of first-order conditioning, he also recognized the importance of mechanisms that allow multiple cues to predict outcomes[12,13]. This type of higher-order conditioning includes sensory preconditioning and second-order conditioning (SOC). The preexposure to paired neutral stimuli (CS1 and CS2) prior to any US exposure permits subsequent CS1-US association to be transferred from one stimulus to another in sensory preconditioning[14]. In contrast, with SOC, the CS2 is associated with CS1 after the first-order conditioning (CS1 paired with US)[15]. While SOC has been established in various organisms, including *Drosophila*, rats, and humans [15–17], it has surprisingly not been verified in mice, despite the availability of various genetic models that can lead to cellular and molecular mechanisms of SOC. Studies using rats demonstrated that infusions of NMDA antagonists or muscimol into the basolateral amygdala (BLA) interfere with the acquisition of SOC[18,19]. The activity within the BLA is pivotal for SOC consolidation as evidenced by the impact of post-training protein synthesis inhibition[20,21] or local anesthesia within the BLA[22]. Furthermore, impairing BLA function hinders the extinction of second-order fear memory[19,23]. Additional research highlights the involvement of dopamine and opioid systems in SOC[24,25].

Sensory preconditioning and SOC serve as suitable paradigms for testing complex learning because they are also prevalent in natural environments[13,17]. In this study, we focused on SOC because CS1 already carries learned value when paired with CS2 thereby providing more salience to associate CS2 with CS1, promoting a CS2-induced conditioned response even though CS2 was never paired directly with US. The first-order memory networks are presumably engaged to propagate the value (aversive or appetitive) to CS2 during SOC[10]. Despite the well-known reactivation of neural networks upon re-exposure to learned CS[26–28], the role of US pathways in SOC remains unknown.

The parabrachial nucleus (PBN) in the dorsal pons receives sensory signals from the periphery and projects to multiple forebrain regions including the central nucleus of the amygdala (CeA)[29–33], which is a primary outlet of the amygdala transmitting fear-related information[34,35]. A subset of PBN neurons expressing the *Calca* gene, encoding calcitonin-gene related peptide ($CGRP^{PBN}$ neurons), is activated by a wide range of aversive and painful stimuli such as foot shock, visceral malaise, and noxious olfactory, gustatory, visual, or auditory stimuli[33,36–44]. Due to this broad tuning to aversive stimuli, these neurons serve as a general alarm for alerting animals to potential danger[40,43,44]. Activation of $CGRP^{PBN}$ neurons via chemogenetic or optogenetic tools evokes a range of aversive unconditioned responses, such as freezing, anorexia, bradycardia, and signs of anxiety[37–39,41,42]. Transient or permanent silencing of these neurons during first-order conditioning attenuates conditioned responses, highlighting their crucial role in the acquisition and expression of aversive, first-order memories[38,41,42]. Notably, $CGRP^{PBN}$ neurons become activated by a tone CS previously paired with a foot shock US, or by a novel taste CS paired with visceral malaise US[40,41].

The reactivation of $CGRP^{PBN}$ neurons by a CS is comparable to the well-known activation of

dopamine neurons by the CS after appetitive learning with a CS-reward pairing[45–47]. Considering that $CGRP^{PBN}$ neurons normally serve to relay the aversive US, their reactivation by CS1 could serve as a surrogate US when paired with a new CS2. The appearance of $CGRP^{PBN}$ neuronal activity after learning provided the incentive for studying the role of $CGRP^{PBN}$ neurons in SOC. Therefore, we aimed to investigate the potential role of $CGRP^{PBN}$ neurons in SOC by developing a behavioral paradigm in mice and using single-cell, calcium imaging of $CGRP^{PBN}$ neurons to monitor dynamic changes in their activity during SOC. We also traced the activity of the same individual neurons over the course of the study. Additionally, to ascertain the critical role of $CGRP^{PBN}$ neurons in SOC, we chemogenetically inhibited these neurons during CS2-CS1 association phase.

Results

Development of a second-order conditioning paradigm for mice

We implemented a second-order fear-conditioning protocol, consisting of four sequential phases across successive days: habituation, first-order association (CS1-US pairing), second-order association (CS2-CS1 pairing), and testing for the conditioned freezing response to CS2 (Fig. 1a). On the first day, mice were habituated to 10 lights (first-order CS) and 10 tones (second-order CS) with random orders. The next day, the mice received 10 trials of light CS1 (10 s, 60 lux) that co-terminated with a foot shock US (0.5 mA, 0.5 s); we measured freezing behavior in response to the light CS1 to document learning (Fig. 1b). On day 3, the mice were exposed four times to tone CS2 (10 s, 70 dB) followed 0.5 s later by the light CS1 to establish a second-order association. The control group (receiving only CS1) did not undergo CS2-CS1 pairing, serving as a baseline for comparison. The number of CS2-CS1 association trials was based on prior rat studies and limited to minimize CS1 extinction[10,19]. Both control and experiment groups exhibited moderate freezing in the chamber without any additional cues, likely due to the contextual fear associated with the chamber from day 2 (Extended Data Fig. 1a). Freezing to the light CS1 increased during the CS2-CS1 pairing reflecting their memory of the association with the US (Fig. 1c). On day 4, the test day, the mice were exposed to the tone CS2 three times (120 s apart) in a novel context to test second-order memory (Fig. 1a). The mice exhibited significant freezing levels to the tone CS2 compared to the control group (Fig. 1d). The percentage of time freezing to the tone CS2 was lower than to the light CS1 on the CS2-CS1 pairing phase. Specifically, the comparison of second-order memory strength to first-order memory averaged around 66.4% across three experiments involving 15 mice (Extended Data Fig. 1b).

Given that first-order conditioning to a specific CS not only elicits conditioned responses directly to that CS but also shows stimulus generalization—where conditioned responses extend to similar stimuli[48,49]—we explored this phenomenon in the context of SOC. After establishing a second-order fear memory for CS2 (a 5-kHz tone, as used in our initial experiment), mice were presented with

103 either the novel 10-kHz novel or the 5-kHz tone CS2 on the test day. Mice showed less freezing to 10-
104 kHz tone than a 5-kHz tone, indicating that mice could distinguish between these tones after SOC (Fig.
105 1e). This result suggests that the second-order memory is not generalized to similar types of stimuli
106 under these experimental conditions.

107 Considering that the mice were exposed to the same context (metal chamber with an electric
108 grid) during both first- and second-order associations, it is possible that the context itself might
109 contribute to the second-order association, either instead of or in addition to the light CS1 because the
110 context CS is capable of evoking contextual fear responses[23,50]. Therefore, the mice might freeze in
111 response to the tone CS2 on the test day due to developing an association between the context and the
112 tone CS2, rather than between the tone CS2 and the light CS1. To test this possibility, we performed an
113 experiment by using the metal chamber only during CS1-US pairing phase and conducting CS2-CS1
114 pairing in a different context. We observed that the mice still displayed a high level of freezing to the
115 tone CS2 in this modified protocol, which indicates that tone CS2 evokes freezing response through the
116 association with the light CS1 (Fig. 1f, control and experiment).

117 In first-order conditioning, the initially neutral CS1 becomes a predictive signal of the US after
118 learning[46,51]. Therefore, we hypothesized that the second-order association is formed only when CS2
119 precedes CS1. To investigate the impact of the timing of CS2 presentation during second-order
120 association, we introduced CS2 in various temporal configurations. In this experiment, different groups
121 of mice were exposed to simultaneous presentation, reversed order of presentation, or with a 30-s
122 interval between the tone CS2 and light CS1 rather than 0.5 s (Fig. 1f). All these groups of mice failed
123 to acquire a fear memory to the tone CS2, in contrast to the experimental group that received the tone
124 CS2 followed by the light with a 0.5-s interval (Fig. 1f). Taken together, these results reveal that mice
125 efficiently associate the fear response to CS2 when CS2 precedes CS1 with a short interval between
126 them.

127 To further optimize SOC paradigm, we asked whether repeating first and second-order
128 associations could enhance conditioned responses to CS2. A group of mice underwent the CS1-US and
129 CS2-CS1 pairing phases as usual, then this sequence was repeated on the next 2 days. After that, they
130 received the tone CS2 to examine second-order fear memory (Fig. 1g, 2-SOC) and mice with the
131 standard protocol (Fig. 1g, experiment). Freezing time in mice with two conditioning trials was not
132 significantly different than the mice with only one (Fig. 1g). Given the importance of memory
133 consolidation in the development of long-term memory in associative learning[52–54], we also tested
134 whether the second-order memory relies on a consolidation period. All mice received the same
135 habitation, followed by different training protocols: the standard 3-day protocol, a 2-day protocol with
136 CS2-CS1 pairing and testing occurring 1 h later, or a 1-day protocol with US-CS1, CS2-CS1 and
137 testing all conducted on the same day (Fig. 1h). Interestingly, only mice that received the 3-day training

protocol demonstrated a significant second-order memory compared to the other groups (Fig. 1i). These findings indicate that SOC requires a period for memory consolidation, such as overnight, to effectively form second-order memories.

We posited that second-order memories might extinguish more rapidly than first-order memories, reflecting their relative weaker conditioned responses. To test this, mice were exposed to an extended series of 10 light CS1 and tone CS2 trials in first-order conditioning and SOC groups, respectively. The mice extinguished their freezing responses to the tone CS2 faster than to the light CS1 (Extended Data Fig. 1c), a result consistent with the slow extinction of the first-order fear memory in previous studies[40].

Sensory preconditioning has a similar experimental procedure to SOC but the CS2-CS1 pairing occurs before the CS1-US pairing. We habituated mice to light CS1 and tone CS2. On day 2, mice received 4 CS2-CS1 pairings with a 0.5-s interval between CS2 offset and CS1 onset. The next day, there were 10 CS1-US pairings. On day 4, we tested their freezing response to light CS1 and tone CS2; the mice received 3 trials of tone CS2 then 3 trials of light CS1. A control group did not receive the CS2 on day 2. Both the sensory preconditioning and control groups had similar learning curves (Extended Data Fig. 1d). Both groups showed a high freezing level to light CS1 on the test day; however, the response to tone CS2 was not different from the control group (Extended Data Fig. 1e, f). These results indicate that while the formation of first-order memory was successful, sensory preconditioning failed to materialize, likely because the four CS2-CS1 paired trials were insufficient to establish a robust CS2-CS1 association necessary for CS2 to elicit a fear memory through its connection to the CS1-US association.

Imaging neuronal activity of CGRP^{PBN} neurons during second-order conditioning

We hypothesized that CGRP^{PBN} neurons would be activated by the tone CS2 after SOC like their reactivation by the light CS1 after first-order conditioning. To observe CGRP^{PBN} neuronal activity across different phases of the SOC protocol, we used calcium imaging in freely behaving mice by injecting AAV-DIO-GCaMP6m (a proxy indicator of neuronal activity[55]) into the PBN of *Calca*$^{Cre/+}$ mice and implanting a GRIN lens over external lateral region of the PBN (Fig. 2a, b and Extended Data Fig. 2a, b). After allowing 4-6 weeks for GCaMP6 expression and stabilization of the imaging field (Fig. 2c), the mice were habituated to the light CS1 and tone CS2. Variability in the number of neurons imaged each day was due to motion and changes in the field of view caused by reattaching the microscope. We confirmed that 8 mice (both sexes) included in the analysis exhibited a significant freezing to tone CS2 after SOC compared to baseline, which was the first 5 min in the chamber before the session started (Fig. 2d). During habituation (day 1), the average fluorescence of CGRP^{PBN} neurons (199 neurons imaged) did not change to the tone or light (Fig. 2e, f). On day 2, the mice were presented

173 with 10 trials of a light CS1 that co-terminated with a foot shock US. Among 103 neurons imaged on
174 day 2, 80.6% of $CGRP^{PBN}$ neurons responded (average of all 10 trials) robustly after foot shock as
175 shown before[40] (Fig. 2g, h). The average fluorescence of $CGRP^{PBN}$ neurons did not increase in response
176 to light CS1 during the early trials (1-3) of first-order association, but there was a trend towards
177 increased activity in trials 8-10 (Extended Data Fig. 2c), which became pronounced the next day. This
178 delayed pattern suggests the need for a consolidation period for the neuronal response to the CS1 to
179 become established.

180 On day 3, mice were exposed to 4 trials of the tone CS2 and light CS1 spaced by 0.5 s.
181 Consistent with previous findings[40,41], we observed that $CGRP^{PBN}$ neurons were activated by the light
182 CS1 even in the absence of the foot shock US. Out of 199 neurons imaged, 43.7% of the $CGRP^{PBN}$
183 neurons were activated by light CS1 and 27.4% of the neurons were activated by tone CS2 (Fig. 2i, j)
184 with no significant difference in response to tone CS2 across the trials (Extended Data Fig. 2d). On the
185 test day, we assessed both freezing level and fluorescent activities of $CGRP^{PBN}$ neurons in response to
186 tone CS2. The average fluorescence of these neurons increased during the tone CS2 presentation.
187 Among 209 $CGRP^{PBN}$ neurons imaged on the test day, 41.4% were activated by the tone CS2, while
188 52.9% showed no response, and 5.7% were inhibited (Fig. 2k, l). Interestingly, the fluorescent activity
189 was sustained for 10 s after the tone CS2 terminated (Fig. 2l). These results reveal that $CGRP^{PBN}$ neurons
190 are innately responsive to the US and become activated in response to CS1 after first-order conditioning
191 and to CS2 after SOC. This progression underscores $CGRP^{PBN}$ neurons' adaptability in associating both
192 direct and indirect cues with aversive stimuli.

193 We analyzed overall neuronal activities of $CGRP^{PBN}$ neurons during SOC procedure by
194 calculating area under the curve (AUC) of traces in response to the two conditioned stimuli. The light
195 CS1 evoked a significant increase of responses during and after pairing with US compared to the
196 habituation phase (Fig. 3a, left). The tone CS2 showed increased activity after SOC rather than during
197 learning phase, compared to the responses before learning (Fig. 3a, right). The average AUC of neurons
198 and freezing in individual mice during tone CS2 in test phase exhibited a significant, but moderate linear
199 correlation (Extended Data Fig. 2e). Using K-means clustering, we identified 5 distinct categories of
200 $CGRP^{PBN}$ neuronal activities among 209 neurons in test phase (Fig. 3b, c). $CGRP^{PBN}$ neurons displayed
201 different peak timings within the analysis window (Fig. 3c). The first cluster (31 neurons, 14.8%)
202 exhibited a large response broadly tuned to tone CS2; they increased their activity during the tone CS2
203 presentation and gradually declined during the 10 s after the tone ceased. The second cluster (46 neurons,
204 22.0%), showed no response during the tone CS2 but started to increase after tone. The third cluster (61
205 neurons, 29.2%) exhibited a small, delayed increase of activity during tone CS2 then returned to
206 baseline. The fourth cluster (55 neurons, 26.3 %) had increased activity at the onset of tone CS2 that
207 gradually dissipated during tone presentation. The last cluster (16 neurons, 7.7%) showed no responses
208 within a window of analysis. Similarly, clustering of $CGRP^{PBN}$ neurons showed dynamic responses

during CS2-CS1 pairing phase (Extended Data Fig. 3a). Three clusters showed robust responses to the light CS1. Another cluster showed a small increase to tone CS2 then a decrease during light CS1. However, during CS1-US pairing, all of clusters showed similar pattern of strong foot shock US response (Extended Data Fig. 3b). This heterogeneity of neuronal responses in CS2-CS1 and test phases may contribute to the complex neural representation of fear-related information during SOC.

To address how the activity of individual $CGRP^{PBN}$ neurons changes across the behavioral paradigm, we traced 122 neurons across phases of the SOC procedure (habituation, CS2-CS1, and test days). Due to motion artifacts caused by the foot shocks, we were unable to include CS1-US pairing phase data in longitudinal registration process of neural activities. Within this set of neurons, we tracked activity changes in response to tone CS2 across days (Fig. 3d). Only 14.8% of neurons were activated to the tone before SOC (habituation); they exhibited a significant decrease in activity (measured as AUC) during and after learning process (Fig. 3e). Most neurons (62.3%), which were unresponsive to the tone CS2 prior to learning, showed significant increase following SOC (Fig. 3f). Another group of neurons, which showed decreased fluorescence in response to tone CS2 before SOC, showed an increase in AUC during and after the SOC procedure (Fig. 3g). These data suggest that the $CGRP^{PBN}$ neurons responsive to the CS2 were mainly derived from those that did not initially respond to the CS2 before learning.

We next examined which $CGRP^{PBN}$ neurons encode first and second-order memory. Among 122 neurons, 53 neurons (43.4%) were responsive during second-order memory recall (Fig. 3h). We asked whether they were the same neurons that were activated by first-order memory (light CS1). Of the 53 neurons responding tone CS2, 47.2% (25 neurons) also responded to light CS1 (CS1/CS2-encoding), the rest of them only responded to CS2 (CS2-encoding, Fig. 3h). The average trace of CS1/CS2-encoding neurons during light CS1 was greater than CS2-encoding neurons (Fig. 3i). The CS1/CS2-encoding neurons showed 1.9 times greater AUC during first-order memory recall compared to second-order memory (Fig. 3j). Also, CS1/CS2-encoding neurons displayed similar AUC to tone CS2 exposure compared to the new CS2-encoding neurons that displayed a broader but sustaining activity even after CS2 (Fig. 3k, l). These results indicate that about half of CS2 responsive $CGRP^{PBN}$ neurons respond to both first and second-order memory and exhibited larger responses to the first-order memory than the second-order memory.

To further assess the impact of SOC on neuronal activity patterns, we calculated the maximum correlation among 122 traced neurons using Pearson's correlation test (Extended Data Fig. 3c, d). On the habituation day, the correlations among neurons in response to tone CS2 were comparable to those observed during the baseline period (5 min before the session started) (Extended Data Fig. 3e, g). However, after the acquisition of the second-order memory, $CGRP^{PBN}$ neurons exhibited a significant increase in maximum correlation in response to tone CS2 compared to the baseline (Extended Data Fig. 3f, h). These results indicate that the acquisition of SOC by a conditioned stimulus alters both the scale

244 and coherence of neuronal activity patterns.

245

246 **Inhibition of CGRP^{PBN} neurons during CS2-CS1 pairing attenuates second-order conditioning**

247 To investigate the necessity of CGRP^{PBN} neurons in SOC, we bilaterally injected AAV-DIO-hM4Di-
248 mCherry, an inhibitory G-protein coupled receptor[56,57], or AAV-DIO-mCherry as a control, into the PBN
249 of *Calca*$^{Cre/+}$ mice (Fig. 4a). After allowing 4 weeks for viral expression, the mice were exposed to the
250 habituation and CS1-US pairing phase followed by an intraperitoneal (i.p.) injection of saline. The next
251 day, the mice received the hM4Di ligand, Clozapine-N-Oxide (CNO, 5 mg/kg, i.p.), 30 min before the
252 CS2-CS1 pairing. On the test day, the freezing response to the tone CS2 was measured (Fig. 4b). The
253 inhibition of CGRP^{PBN} neurons via CNO treatment did not affect freezing responses during the CS2-
254 CS1 pairing compared to controls (Fig. 4c). However, chemogenetic inhibition of CGRP^{PBN} neurons
255 during the second-order association resulted in a significant (44.2%) reduction in the freezing level to
256 tone CS2 on the test day, compared to both the mCherry-control group (Extended Data Fig. 4a) and the
257 experimental group (WT mice experiment in Fig. 1) trained with the standard SOC protocol (Extended
258 Data Fig. 4b). Additionally, the hM4Di group exhibited a decreased freezing response after the 10-s
259 tone CS2 presentation compared to the control group (Extended Data Fig. 4c). The freezing response
260 of the hM4Di group to tone CS2 was only 32.2% of their response to light CS1, indicating a diminished
261 strength of second-order memory compared to the 66.4% observed in the standard protocol (Fig. 4d).
262 These results indicate that activity of CGRP^{PBN} neurons contributes significantly to the second-order
263 association.

264

265 **Discussion**

266 We established a SOC paradigm in mice employing an aversive stimulus and two distinct sensory cues.
267 Our findings demonstrate the ability of mice to form second-order association, following first-order
268 conditioning, in the absence of the US. Through one-photon, calcium imaging of CGRP^{PBN} neurons *in*
269 *vivo*, we characterized their dynamic responses throughout the learning progression. Initially, these
270 neurons were activated exclusively by the US. However, after the CS1 was paired with the US, they
271 began responding to CS1. While there was no increase in average response to CS2 during CS2-CS1
272 pairing phase, a significant 41.1% of CGRP^{PBN} neurons showed a strong response to CS2 on the
273 subsequent, test day. Longitudinal tracking of neuronal activity revealed that the CS2-encoding
274 CGRP^{PBN} neurons emerged from both the CS1-encoding population and neurons that were unresponsive
275 before learning. Furthermore, chemogenetic inhibition of CGRP^{PBN} neurons during the second-order
276 association phase led to a decrease in fear responses to CS2. This finding highlights the dual role of
277 CGRP^{PBN} neurons: they are crucial for transmitting signals about the US and for encoding information

about environmental cues that predict aversive events.

Higher-order conditioning, while not as extensively studied as first-order conditioning, likely plays a significant role in natural environments resembling the complexity of human memory formation[58]. It is well-documented that in first-order classical conditioning, the learning efficiency is maximized when the CS precedes the US[59,60]. Similarly, the present study demonstrated that successful second-order association occurs when CS2 is presented before CS1. Furthermore, we found that for SOC to be effective, the interval between CS2 and CS1 needs to be short.

We have identified several distinctive features of SOC compared to first-order conditioning. One notable difference is the weaker strength of second-order memory compared to first-order memory, evidenced by freezing levels to CS2 being around 66.4 % of those elicited by CS1. This disparity likely arises from the absence of the US during CS2-CS1 pairing, leading to a less potent valence attributed to the second-order association. This feature may also contribute to faster extinction of second-order memory compared to first-order memory. Given similar extinction patterns observed in experiments with tone CS1 and light CS2 in rats[19], the faster extinction of second-order memory to tone CS2 in our study may not be due to sensory modality differences between the light and tone. The moderated strength of second-order memory might afford animals greater flexibility in their responses in a changing environment.

The absence of a US during the association of CS2 with CS1 can be compared to a prediction error, a fundamental concept in associative learning theory, which posits the discrepancy between real and expected outcomes as a key driver of learning[46,47,51]. Maes et al. showed that second-order memory is disrupted when midbrain dopamine neurons are inactivated at the start of the reward-predicting cue[61]. Dopamine neurons in ventral tegmental area (VTA) are known to be activated by omission of the US during fear extinction[47,62]. Also, dopamine neurons innervate the BLA and promote second-order fear conditioning via the dopamine D1 receptor[24]. Infusion of a NMDAR antagonist in BLA is critical for acquisition of second-order memory when the expected shock is omitted[63]. $CGRP^{PBN}$ neurons may play a similar role in aversive learning as dopamine neurons play in appetitive learning. Activation of parabrachial neurons has been found to inhibit dopamine neurons in the VTA[64,65] and although $CGRP^{PBN}$ neurons do not project directly to the VTA, they might exert an indirect influence. Hence, $CGRP^{PBN}$ neurons could also contribute to aversive learning by inhibiting the activity of VTA dopamine neurons.

Sensory preconditioning, a variant of higher-order conditioning, was not strongly established under our test conditions, possibly due to an insufficient number of CS2-CS1 paired trials required to establish an association[10,19]. During the CS2-CS1 pairing phase, these conditioned stimuli had no inherent valance, as CS1 was associated with the US only on the subsequent day. This contrasts with SOC, where $CGRP^{PBN}$ neurons become activated during the CS2-CS1 paired trials due to the prior establishment of CS1-US association.

The calcium activity of $CGRP^{PBN}$ neurons throughout the learning process revealed their role in SOC. Initially, during first-order conditioning, these neurons respond robustly to the US but showed no significant reaction to the CS1. However, by the following day, they became responsive to the CS1 during CS2-CS1 association, indicating that they are recruited during memory formation, which apparently requires a consolidation period. Given the role of $CGRP^{PBN}$ neurons as a general alarm[44], their reactivation by the CS1 could effectively generate alarm signals, acting as a surrogate US during the association with CS2. Hence, the reactivation of the US pathway by CS after learning provides insights into the neural mechanisms of higher-order conditioning. There are at least two hypotheses for what drives $CGRP^{PBN}$ neuron responses to a CS after learning. Since these neurons are known to respond to aversive sensory stimuli[44], one possibility is that signaling pathways from the CS1 to the $CGRP^{PBN}$ neurons is potentiated through conditioning process. Alternatively, as the association between the CS and US is consolidated, the presentation of CS might elicit physiological responses that resemble those triggered by the US (e.g. foot shock) itself[42].

Cluster analysis revealed diverse activity patterns of $CGRP^{PBN}$ neurons in response to the CS2. Three of the clusters responded to the CS2, potentially involved in encoding learned CS2 (clusters 1, 3, 4). Two clusters exhibited activity following the tone (clusters 1, 2). Considering the heterogeneity of CGRP-expressing neurons in the PBN[66,67] these distinct sub-populations likely process and encode CS and US information in diverse ways. Future studies exploring the gene expression profiles of these clusters could provide deeper insights into their functional roles and contributions to associative learning processes.

Longitudinal tracking of neurons revealed activity changes within $CGRP^{PBN}$ neurons throughout the learning process. Most of the neurons were activated in response to the US, as expected. After first-order conditioning, 43.7% of neuronal population was activated by CS1; about half of them became responsive to the tone CS2 on the test day. Because the CS1/CS2-encoding $CGRP^{PBN}$ neurons had a larger response (AUC) during CS1 than CS2, they may correlate best with the robustness of freezing behavior. Selective manipulation of this distinct population, while challenging, could yield valuable insights into their specific role in neural ensemble of first- and second-order associative memories.

Chemogenetic inhibition of $CGRP^{PBN}$ neurons during CS2-CS1 association attenuated second-order memory. Similar attenuation of first-order memory was observed in previous experiments that transiently inhibited this US pathway during foot shock[42]. The partial attenuation is presumably due to redundant US pathways mediating aversive learning, such as the amygdala, deep cerebellar nuclei, and basal forebrain[68,69]. Intriguingly, the inhibited group of mice exhibited reduced freezing levels not only during CS2 but also 10 s later. This observation aligns with the increased calcium activity detected in some $CGRP^{PBN}$ neurons both during and after CS2 exposure on the test day. Such sustained neuronal activity post-CS2 suggests that it plays a significant role in maintaining the freezing response following

CS2.

Emerging evidence demonstrates the reactivation of the US pathway neurons by the CS after first-order conditioning. $CGRP^{PBN}$ neurons, for instance, are activated by the cue after both fear and taste learning[40,41]. Likewise, foot shock-responding deep cerebellar nuclei neurons projecting to PBN exhibited increased activity during re-exposure to the CS after fear conditioning[69]. In the basal forebrain, neurons expressing choline acetyltransferase (ChAT) and projecting to basolateral amygdala (BLA) displayed similar activity changes after learning and inhibiting them during or after learning attenuated conditioned responses to the CS[70]. $CGRP^{PBN}$ neurons project axons to the basal forebrain (nucleus basalis or substantia innominata)[67]. This suggests that $CGRP^{PBN}$ neurons could drive the activity of ChAT neurons in the basal forebrain, thereby facilitating associative learning. Furthermore, the reactivation of $CGRP^{PBN}$ neurons after learning sheds light on the neural mechanisms of higher-order conditioning, elucidating how conditioned stimuli can be associated with each other without an actual US. Unraveling the neural mechanisms of higher-order fear conditioning may provide further insights into the treatment of fear and anxiety-related disorders.

References

1. Rogan, M. T., Staubli, U. V. & LeDoux, J. E. Fear conditioning induces associative long-term potentiation in the amygdala. *Nature* **390**, 604-607 (1997).

2. Armony, J. L., Servan-Schreiber, D., Cohen, J. D. & LeDoux, J. E. An Anatomically Constrained Neural Network Model of Fear Conditioning. *Behav. Neurosci.* **109**, 246–257 (1995).

3. Delgado, M. R., Nearing, K. I., LeDoux, J. E. & Phelps, E. A. Neural Circuitry Underlying the Regulation of Conditioned Fear and Its Relation to Extinction. *Neuron* **59**, 829–838 (2008).

4. Johansen, J. P., Cain, C. K., Ostroff, L. E. & Ledoux, J. E. Molecular Mechanisms of Fear Learning and Memory. *Cell* **147**, 509–524 (2011).

5. Kim, J. J. & Thompson, R. F. Cerebellar circuits and synaptic mechanisms involved in classical eyeblink conditioning. *Trends. Neurosci.* **20**, 177–181 (1997).

6. Robleto, K., Poulos, A. M. & Thompson, R. F. Brain Mechanisms of Extinction of the Classically Conditioned Eyeblink Response. *Learn. Mem.* **11**, 517–524 (2004).

7. Yau, J. O. Y. & McNally, G. P. Brain mechanisms controlling Pavlovian fear conditioning. *J Exp Psychol Anim Learn. Cogn.* **44**, 341–357 (2018).

8. Kim, J. J. & Jung, M. W. Neural circuits and mechanisms involved in Pavlovian fear conditioning: A critical review. *Neurosci. Biobehav. Rev.* 30, 188–202 (2006).

9. Holmes, N. M., Fam, J. P., Clemens, K. J., Laurent, V. & Westbrook, R. F. The neural substrates of higher-order conditioning: A review. *Neurosci. Biobehav. Rev.* 138:104687 (2022).

10. Gostolupce, D., Lay, B. P. P., Maes, E. J. P. & Iordanova, M. D. Understanding

Associative Learning Through Higher-Order Conditioning. *Front. Behav. Neurosci.* **16**, 16:845616 (2022).

11. Bolles, R. C. & Collier, A. C. The effect of predictive cues on freezing in rats. *Anim Learn. Behav.* **4**, 6–8 (1976).

12. Pavlov, I. P. Conditioned reflexes: an investigation of the physiological activity of the cerebral cortex. *Oxford Univ. Press* (1927).

13. Brogden, W. J. Higher Order Conditioning. *Amer. J. Psych.* **52**, 579-591 (1939).

14. Brogden, W. J. Sensory Pre-conditioning. *J. Exp. Psych.* **25** (1939).

15. Rizley, R. C. & Rescorla, R. A. Associations in Second-Order Conditioning and Sensory Preconditoning. *J. Comp. Physiol. Psychol.* **81**, 1-11 (1972).

16. Tabone, C. J. & De Belle, J. S. Second-order conditioning in Drosophila. *Learn. Mem.* **18**, 250–253 (2011).

17. Lee, J. C. Second-Order Conditioning in Humans. *Front. Behav. Neurosci.* **15**, 672628 (2021).

18. Parkes, S. L. & Westbrook, R. F. Role of the basolateral amygdala and NMDA receptors in higher-order conditioned fear. *Rev. Neurosci.* **22** 317–333 (2011).

19. Parkes, S. L. & Westbrook, R. F. The basolateral amygdala is critical for the acquisition and extinction of associations between a neutral stimulus and a learned danger signal but not between two neutral stimuli. *J. Neurosci.* **30**, 12608-12618 (2010).

20. Williams-Spooner, M. J., Westbrook, R. F. & Holmes, N. M. The Conditions under Which Consolidation of Serial-Order Conditioned Fear Requires De Novo Protein Synthesis in the Basolateral Amygdala Complex. *J. Neurosci.* **39**, 7357–7368 (2019).

21. Leidl, D. M., Lay, B. P. P., Chakouch, C., Westbrook, R. F. & Holmes, N. M. Protein synthesis in the basolateral amygdala complex is required for consolidation of a first-order fear memory, but not for consolidation of a higher-order fear memory. *Neurobiol. Learn. Mem.* **153**, 153–165 (2018).

22. Lay, B. P. P., Westbrook, R. F., Glanzman, D. L. & Holmes, N. M. Commonalities and Differences in the Substrates Underlying Consolidation of First- and Second-Order Conditioned Fear. *J. Neurosci.* **38**, 1926–1941 (2018).

23. Lingawi, N. W., Laurent, V., Westbrook, R. F. & Holmes, N. M. Acquisition and extinction of second-order context conditioned fear: Role of the amygdala. *Neurobiol. Learn. Mem.* **183**, 107485 (2021).

24. Nader, K. & LeDoux, J. E. Inhibition of the mesoamygdala dopaminergic pathway impairs the retrieval of conditioned fear associations. *Behav. Neurosci.* **113**, 891–901 (1999).

25. Michalscheck, R. M. L., Leidl, D. M., Westbrook, R. F. & Holmes, N. M. The Opioid Receptor Antagonist Naloxone Enhances First-Order Fear Conditioning, Second-Order Fear Conditioning and Sensory Preconditioning in Rats. *Front. Behav. Neurosci.* **15**, 771767 (2021).

26. Maren, S. Neurobiology of Pavlovian Fear Conditioning. *Annu. Rev. Neurosci.* **24**, 897-931 (2001).

27. Iwata, J. & LeDoux, J. E. Dissociation of Associative and Nonassociative Concommitants of Classical Fear Conditioning in the Freely Behaving Rat. *Behav. Neurosci.* **102**, 66–76 (1988).

28. Goosens, K. A. & Maren, S. Contextual and Auditory Fear Conditioning are Mediated by the Lateral, Basal, and Central Amygdaloid Nuclei in Rats. *Learn. Mem.* **8**, 148-155 (2001).

29. Tokita, K., Inoue, T. & Boughter, J. D. Afferent connections of the parabrachial nucleus in C57BL/6J mice. *Neuroscience* **161**, 475-488 (2009).

30. Chiang, M. C. *et al.* Divergent Neural Pathways Emanating from the Lateral Parabrachial Nucleus Mediate Distinct Components of the Pain Response. *Neuron* **106**, 927-939 (2020).

31. Saper, C. B. & Loewy, A. D. Efferent connections of the parabrachial nucleus in the rat. *Brain. Res.* **197**, 291-317 (1980).

32. Han, W. *et al.* A Neural Circuit for Gut-Induced Reward. *Cell* **175**, 665-678 (2018).

33. Roman, C. W., Derkach, V. A. & Palmiter, R. D. Genetically and functionally defined NTS to PBN brain circuits mediating anorexia. *Nat. Commun.* **7**, 11905 (2016).

34. Lee, S., Kim, S.-J., Kwon, O.-B., Lee, J. H. & Kim, J.-H. Inhibitory networks of the amygdala for emotional memory. *Front. Neural. Circuits.* **7**, 129 (2013).

35. Pare, D. & Duvarci, S. Amygdala microcircuits mediating fear expression and extinction. *Curr. Opin. Neurobiol.* **22**, 717–723 (2012).

36. Carter, M. E., Soden, M. E., Zweifel, L. S. & Palmiter, R. D. Genetic identification of a neural circuit that suppresses appetite. *Nature* **503**, 111–114 (2013).

37. Carter, M. E., Han, S. & Palmiter, R. D. Parabrachial calcitonin gene-related peptide neurons mediate conditioned taste aversion. *J. Neurosci.* **35**, 4582-4586 (2015).

38. Han, S., Soleiman, M., Soden, M., Zweifel, L. & Palmiter, R. D. Elucidating an Affective Pain Circuit that Creates a Threat Memory. *Cell* **162**, 363–374 (2015).

39. Campos, C. A. *et al.* Cancer-induced anorexia and malaise are mediated by CGRP neurons in the parabrachial nucleus. *Nat. Neurosci.* **20**, 934–942 (2017).

40. Campos, C. A., Bowen, A. J., Roman, C. W. & Palmiter, R. D. Encoding of danger by parabrachial CGRP neurons. *Nature* **555**, 617–620 (2018).

41. Chen, J. Y., Campos, C. A., Jarvie, B. C. & Palmiter, R. D. Parabrachial CGRP Neurons Establish and Sustain Aversive Taste Memories. *Neuron* **100**, 891-899.e5 (2018).

42. Bowen, A. J. *et al.* Dissociable control of unconditioned responses and associative fear learning by parabrachial CGRP neurons. *Elife* **9**, 59799 (2020).

43. Kang, S. J. *et al.* A central alarm system that gates multi-sensory innate threat cues to the amygdala. *Cell Rep.* **40**, 111222 (2022).

44. Palmiter, R. D. The Parabrachial Nucleus: CGRP Neurons Function as a General Alarm. *Trends Neurosci.* **41** 280–293 (2018).

45. Schultz, W. Getting Formal with Dopamine and Reward. *Neuron* **36**, 241–263 (2002).

46. Schultz, W., Dayan, P. & Montague, P. R. A neural substrate of prediction and reward.

Science **275**, 1593–1599 (1997).

47. Iordanova, M. D., Yau, J. O. Y., McDannald, M. A. & Corbit, L. H. Neural substrates of appetitive and aversive prediction error. *Neurosci. Biobehav. Rev.* **123**, 337 (2021).

48. Dunsmoor, J. E. & Paz, R. Fear Generalization and Anxiety: Behavioral and Neural Mechanisms. *Biol. Psychiatry.* **78**, 336–343 (2015).

49. Asok, A., Kandel, E. R. & Rayman, J. B. The neurobiology of fear generalization. *Front. Behav. Neurosci.* **12**, 427950 (2019).

50. Debiec, J., LeDoux, J. E. & Nader, K. Cellular and Systems Reconsolidation in the Hippocampus. *Neuron* **36**, 527–538 (2002).

51. Schultz, W. Predictive reward signal of dopamine neurons. *J. Neurophysiol.* **80**, 1–27 (1998).

52. Lee, J. H., Kim, W. Bin, Park, E. H. & Cho, J. H. Neocortical synaptic engrams for remote contextual memories. *Nat. Neurosci.* **26**, 259–273 (2022).

53. Kitamura, T. *et al.* Engrams and circuits crucial for systems consolidation of a memory. *Science* **356**, 73–78 (2017).

54. Dudai, Y., Karni, A. & Born, J. The Consolidation and Transformation of Memory. *Neuron* **88**, 20–32 (2015).

55. Lin, M. Z. & Schnitzer, M. J. Genetically encoded indicators of neuronal activity. *Nat. Neurosci.* **19**, 1142–1153 (2016).

56. Rogan, S. C. & Roth, B. L. Remote Control of Neuronal Signaling. *Pharmacol. Rev.* **63**, 291–315 (2011).

57. Armbruster, B. N., Li, X., Pausch, M. H., Herlitze, S. & Roth, B. L. Evolving the lock to fit the key to create a family of G protein-coupled receptors potently activated by an inert ligand. *Proc. Natl. Acad. Sci. USA* **104**, 5163–5168 (2007).

58. Sepahvand, T., Power, K. D., Qin, T. & Yuan, Q. The Basolateral Amygdala: The Core of a Network for Threat Conditioning, Extinction, and Second-Order Threat Conditioning. *Biology (Basel)* **12**, 1274 (2023).

59. Matzel, L. D., Held, F. P. & Miller, R. R. Information and expression of simultaneous and backward associations: Implications for contiguity theory. *Learn. Motiv.* **19**, 317–344 (1988).

60. Cooper, L. D. Temporal Factors in Classical Conditioning. *Learn. Motiv.* **22**, 129–152 (1991).

61. Maes, E. J. P. *et al.* Causal evidence supporting the proposal that dopamine transients function as temporal difference prediction errors. *Nat. Neurosci.* **23**, 176–178 (2020)

62. Salinas-Hernández, X. I. *et al.* Dopamine neurons drive fear extinction learning by signaling the omission of expected aversive outcomes. *Elife* **7**, 38818 (2018).

63. Williams-Spooner, M. J., Delaney, A. J., Westbrook, R. F. & Holmes, N. M. Prediction Error Determines Whether NMDA Receptors in the Basolateral Amygdala Complex Are Involved in Pavlovian Fear Conditioning. *J. Neurosci.* **42**, 4360–4379 (2022).

64. Coizet, V., Dommett, E. J., Klop, E. M., Redgrave, P. & Overton, P. G. The parabrachial

nucleus is a critical link in the transmission of short latency nociceptive information to midbrain dopaminergic neurons. *Neuroscience* **168**, 263–272 (2010).

65. Yang, H., de Jong, J.W., Cerniauskas, I. et al. Pain modulates dopamine neurons via a spinal–parabrachial–mesencephalic circuit. *Nat. Neurosci.* **24**, 1402–1413 (2021).

66. Nardone, S. *et al.* A spatially-resolved transcriptional atlas of the murine dorsal pons at single-cell resolution. *bioRxiv* 558047 (2023).

67. Pauli, J. L. *et al.* Molecular and anatomical characterization of parabrachial neurons and their axonal projections. *Elife* **11**, 81868 (2022).

68. Crimmins, B. E. *et al.* Basal forebrain cholinergic signaling in the basolateral amygdala promotes strength and durability of fear memories. *Neuropsychopharmacology* **48**, 605-614 (2023).

69. Hwang, K. D. *et al.* Cerebellar nuclei neurons projecting to the lateral parabrachial nucleus modulate classical fear conditioning. *Cell Rep.* **42**, 112291 (2023).

70. Rajebhosale, P. *et al.* Basal forebrain cholinergic neurons are part of the threat memory engram. *bioRxiv* 442364 (2023)

71. Segalin, C. *et al.* The mouse action recognition system (MARS) software pipeline for automated analysis of social behaviors in mice. *Elife* **10**, 63720 (2021).

72. Franklin, K. and Paxinos G. *et al.* Paxinos and Franklin's the Mouse Brain in Stereotaxic Coordinates; 5th edition. *Academic Press*, (2019).

Author contribution

R.P. and S.P. designed research and wrote manuscript; S.P and A.Z. performed and analyzed behavioral experiments; S.P. and F.C. performed and analyzed 1-photon imaging; A.Z. generated customized code for data extraction; S.P and F.C analyzed Ca^{2+} imaging data.

Acknowledgments

We thank Susan Phelps for maintaining the mouse colony, Dr. Larry Zweifel, Dr. Jeansok Kim and lab members for their comments, and Dr. Steve Thomas (University of Pennsylvania) who after a seminar suggested that *Calca* neurons might mediate second-order conditioning.

Data and code availability

541 **Methods**

542 **Animals**

543 All experiments were approved by the University of Washington Institutional Animal Care and Use
544 Committee and were performed under the guidelines described in the US National Institutes of Health
545 Guide for the Care and Use of Laboratory Animals. The behavioral paradigm (Fig. 1) was established
546 using male and female C57BL/6J mice (Jackson Lab #000664) that were 8-12 weeks old. The imaging
547 and hM4Di inhibition experiments were performed with *Calca*$^{Cre/+}$ mice (Jackson Lab #33168) that
548 were generated as described[36] and backcrossed to C57BL/6 mice for >10 generations. Stereotaxic
549 surgeries were performed on males and females when the mice were 8-12 weeks old, and experiments
550 began at least 4 weeks after surgery. Mice were housed on a 12-h light and dark cycle at ~22°C with
551 food and water available ad libitum. Animals from the same litter were split randomly between control
552 and experimental groups, with an nearly equal number of male and female mice in each group. The
553 experiments were not powered to examine sex differences in behavior or CGRP^{PBN} activity, but no
554 differences were apparent.

555

556 **Stereotaxic surgery**

557 Mice were anesthetized with 5% isoflurane and placed on a stereotaxic frame (Neurostar). Isoflurane
558 was maintained 1.5– 2% during the surgical process. For calcium imaging studies *in vivo*, viral
559 injections were into the external lateral region of the PBN using the coordinates; AP -4.90 mm; ML
560 ±1.35 mm; DV +3.40. Viruses were injected unilaterally (randomly assigned) total 0.5 µl at 0.1 µl/min
561 injection speed. A gradient refractive index (GRIN) lens (Inscopix) was placed above target (AP -4.80
562 mm; ML ±1.7 mm; DV +3.65). The lens was lowered at 0.1 mm/min. It included 3 stainless steel wires
563 (0.127 mm bare, uncoated, A-M Systems) that protruded ~0.5 mm beyond the tip; this reduced motion
564 artifacts during imaging. Lens and baseplate for the microscope was secured on the skull with super
565 glue, C&B Metabond (Parkell) and dental cement. After 4 weeks of recovery, mice were tested to check
566 field of view (FOV). Animals with a stable FOV were used in the experiments for the next 2-4 weeks.
567 For chemogenetic manipulation of CGRP^{PBN} neurons, the same coordinates were used for bilateral
568 injection of AAV1-SYN1-DIO-hM4Di-mCherry (Addgene, #44362) or AAV1-DIO-mCherry (Palmiter
569 lab) alone as control. AAV1-Ef1a-DIO-GCaMP6m (Palmiter lab) was injected unilaterally (left or right
570 side were randomly assigned). Mice were allowed to recover for 4 to 5 weeks before the start of
571 behavioral tests. For all experiments, histological verification of targeted viral transduction was
572 documented at the end of the experiments by histological analysis. This was especially important for
573 the hM4Di experiments where adequate bilateral transduction was essential. Only 40% of the mice
574 injected with virus were deemed good hits by a histologist blinded to the treatments.

575 **Higher-order conditioning**

576 All procedures were performed in 28×28×25 cm metal chamber connected to shock grid, controller,
577 light, and speaker (Med Associates). For standard protocol of SOC, mice were habituated to the metal
578 chamber (context A) and given a 10-s CS1 (60 lux light), and CS2 (5 kHz, 70 dB tone) 10 times for 3
579 consecutive days. A block of 10 CS1 consisted with 1 or 2 min of interval between stimuli and a same
580 block of CS2 were delivered in random order across days. The last day of habituation is considered as
581 experimental day 1. On Day 2, mice were placed in the context A for a 10-min of baseline period, then
582 they received 10 CS1 presentations (10 s) that co-terminated with foot shock (0.5 mA, 0.5 s) with 2-
583 min inter-trial interval (ITI). On Day 3, mice were exposed to the context A and received CS2, followed
584 by CS1 0.5 s later. This CS2 and CS1 pairing was repeated 4 times with a 2-min ITI. On day 4, the mice
585 were placed in 28×28×25 cm chamber with acrylic panel walls (context B) for 10 min then received 3
586 10-s CS2 tones with a 2-min ITI. Annotation of freezing was measured manually using Ethovision
587 software (Noldus). Freezing frames were determined manually then Ethovision calculated onset and
588 duration. A control group that was not exposed to CS2 on day 3, which resulted in no association
589 between CS2 and CS1 and served as a background freezing level.

590 For the generalization of SOC experiment, the mice were presented with ten 5 and 10-kHz
591 tones and lights during 3 days of habituation. Day 1 and 2 were the same as the standard protocol, on
592 day 3 the mice received 4 pairings of 5-kHz tone followed 0.5 s later by light. On test day 3, mice
593 received three 10-kHz tones then received three 5-kHz tones to allow a comparison of their responses
594 within each animal.

595 For manipulation of CS2 and CS1 timing experiment, we introduced different patterns of CS2
596 and CS1 to each group of mice. This experiment was conducted in different context setting compared
597 to the standard SOC protocol. To minimize contextual contributions, CS1-US association was
598 conducted in context A, while other phases were conducted in context B. One group received CS2 and
599 CS1 simultaneously (Simultaneous), a second group received CS1 30 s after CS2 (30-s interval), while
600 a third group received CS1 first then CS2 with 0.5 s of interval (Reversed). Control group did not receive
601 CS2 and Experiment group received CS2 then CS1 with 0.5 s of interval. These combinations were
602 conducted 4 times as in the standard procedure above.

603 For the different procedure length experiment, a group of animals underwent the standard SOC
604 protocol (3-day). The 2-day group received the standard procedure until CS1-US phase, then received
605 CS2-CS1 and the test with an hour apart. The 1-day group received CS1-US, CS2-CS1, and the test
606 within the same day with an hour interval between sessions. During the hour interval, mice were in the
607 home cage.

608 For extinction of second-order memory experiment, SOC control and SOC extinction groups
609 of mice went through standard SOC procedure described above except that on day 4 (test day) the mice

610 received 10 trials of CS2 instead of usual 3. Extinction of the CS1 response was also measured for 10
611 trials in different group (FOC extinction) at the next day of CS1-US.

612 Sensory preconditioning procedure was performed by switching day 2 and 3 of SOC procedure.
613 We used the same parameters for shock, CS2 and CS1 for sensory preconditioning. On day 2, both
614 control and experimental mice received CS2-CS1 association (control did not receive CS2), then the
615 CS1-US association was on day 3. On the test day, we exposed mice 3 times to CS2 and CS1 to compare
616 freezing response between groups and conditioned stimuli.

617

618 **Chemogenetic inhibition of CGRP^{PBN} neurons**

619 Clozapine N-oxide (CNO) was prepared in sterile saline and administered intraperitoneally (i.p.). For
620 chemogenetic inhibition of CGRP^{PBN} neurons during SOC experiment, the mice were acclimated to the
621 i.p. injection by receiving i.p. injection of saline (10 µl/g) 30 min before the habituation session for 3
622 consecutive days. On day 1 saline was injected 30 min before the start of session (CS1-US association).
623 Next day, CNO (5 mg/kg at 10 µl/g; RTI#C929) was injected to control and hM4Di group 30 min before
624 the association between CS2 and CS1. On the test day, mice did not receive any injections prior to
625 session. The extent of viral transduction in both left and right PBN was determined histologically (see
626 below) and only those mice with ample transduction (8 of 20 mice) on both sides (judged by someone
627 blind to the experiment) were included in the analysis.

628

629 **Calcium imaging and analysis**

630 After 4 weeks of recovery, mice were habituated to being handled by the experimenter. An nVista
631 microscope (Inscopix) was attached to the baseplate once a week to check FOV. Recording proceeded
632 with IDAS program (Inscopix) and the best e-focus was determined by visual inspection. Sometimes
633 mice received brief air puff to see if CGRP^{PBN} neurons responded to this aversive stimulus. Due to
634 geometrical difficulties of PBN, our success rate of surgery for Ca^{2+} imaging was low with 8 of 20 mice
635 with good neuron visualization. About 26 CGRP^{PBN} neurons were observed per mouse (range 15 to 44).
636 Only mice with >15 neurons in the FOV were used for experiments. For SOC experiments, nVista was
637 connected to test chamber (Med Associates) via BNC cable to receive TTL (Transistor-Transistor-Logic)
638 inputs from test chamber to match the onset and offset of calcium imaging sessions with the video
639 recording. Stimuli onset including foot shock, tone and light were also delivered as TTL to nVista.

640 The imaging parameters were chosen for the least amount of photobleaching, but sufficient
641 fluorescence (LED power, 0.2 - 0.5). Raw data were processed with IDPS software (ver. 1.9.1, Inscopix).
642 After 4X spatial and 2X temporal down sampling, data were processed with spatial bandpass filter to

643 reduce background noise. Then motion correction was applied to the images based on reference frame
644 and region of interest (ROI) in FOV. Principal component analysis/Independent component analysis
645 (PCA/ICA) in IDPS were used to extract ΔF/F of neurons from raw data. Thirteen pixel of average cell
646 diameter, 150 of principal components, 100 ICA maximum iterations were used as parameters to
647 identify cells using PCA/ICA[40]. In some cases, with severe motion and high background, a manual ROI
648 analysis method was applied. The maximum projection images were used as reference of spatial
649 information of neurons, then ROIs were manually drawn based on the boarder of neurons. All neurons
650 were visually inspected for each cell based on shape and dynamics to verify accuracy.

651 For tracking of individual neurons across days were done by using longitudinal registration
652 function of IDPS (minimum correlation, 0.5). After generating cell traces, neurons were manually
653 inspected and removed from analysis when they lost trace some days or captured different neurons
654 within the analysis file.

655 Raw data from IDPS were processed to calculate DF/F and Z score using customized MATLAB code
656 (https://doi.org/10.5281/zenodo.10725342). Since the output of manual ROI analysis was raw data,
657 ΔF/F was calculated as $\Delta F/F = \frac{[(F-mean(F))]}{mean(F)}$. Mean($F$) indicate average F of entire trace. For
658 PCA/ICA analysis, output data were used because the output of PCA/ICA analysis is ΔF/F. For
659 comparison of multiple animals, Z score was used which was calculated as $Z = \frac{[F-mea\ \ (F0)]}{Standard\ deviation(F0)}$.
660 F_0 indicates F between -10 to 0 second. Time 0 indicates any type of stimuli onset (US, CS1, CS2).
661 For classification of neurons, area under the curve (AUC) of ΔF/F during before (-10 to 0 s)
662 and after (0 to 10 s) events of interest were calculated. Neurons with >50% increase of AUC
663 (after/before the event) were classified as 'increased' group of neurons. Neurons >50% decrease of
664 AUC were classified as 'decreased' group. The remaining neurons did not show >50% increase or
665 decrease were classified as a 'no change' group. K-means clustering was performed using Behavior
666 Ensemble and Neural Trajectory Observatory (Bento) which is an open source, calcium-imaging-
667 analysis program developed by D. Anderson and A. Kennedy[71]. Z scored traces from -10 s to +20 s of
668 all animals were used as an input, then K-means clustering performed with group number of 5. Optimal
669 number of clusters was determined using a Silhouette score[71].

670 The correlation analysis of neurons was conducted using version 23.6 of the Inscopix Data
671 Exploration, Analysis, and Sharing (IDEAS, Inscopix) platform. Uploaded traces were analyzed using
672 the "Compare Neural Circuit Correlations Across States" tool within IDEAS. This tool computes
673 maximum pairwise correlations among cell traces within specific states (e.g., baseline, tone, and light).
674 Additionally, it determines the differences in correlations between these states, represented by Cohen's
675 d values.

676 **Histology and Microscopy**

677 Mice were anesthetized with Beuthansia (0.2 ml, i.p.; Merck) and transcardially perfused with
678 phosphate-buffered saline (PBS) followed by 4% paraformaldehyde (PFA, Electron Microscopy
679 Science) in PBS. Then brains were extracted and fixed in 4% PFA at 4°C overnight. The next day, the
680 brains were moved to 30% sucrose for 48 hr. Brains were frozen in OCT compound (ThermoFisher)
681 before sectioning. Coronal stions (30 µm) were made on a cryostat (Leica Microsystems), then stored
682 in PBS. For immunostaining, 30-µm sections were washed in PBS and incubated in the blocking
683 solution (3% normal donkey serum in PBST) for 1 hr at room temperature. Primary antibodies were
684 applied to the solution and incubated overnight in 4 °C: chicken-anti-GFP (1:10000, Abcam, ab13970),
685 and rabbit-anti-DsRed (1:1000, Takara, 632496). After 3 washes in PBS, sections were incubated for 1
686 h in PBS with secondary antibodies: Alexa Fluor 488 donkey anti-chicken (1: 500, Jackson
687 ImmunoResearch, #2340375), Alexa Fluor 594 donkey anti-rabbit (1:500, Jackson ImmunoResearch,
688 #2340621). Then the sections were mounted onto glass slides, and coverslipped with DAPI
689 Fluoromount-G (Southern Biotech). Sections were imaged with a Keyence BZ-X700 microscope.

690

691 **Quantification and statistical analysis**

692 An online power and sample size calculator was used to determine an effective sample size for statistical
693 comparisons (http://powerandsamplesize.com). Prism 9 (GraphPad) was used for all other statistical
694 analysis. For all data, normality was tested using the Shapiro-Wilk test to determine whether parametric
695 or non-parametric analyses were required. For comparing two groups, Student t-test were used
696 otherwise ANOVA (one-way/two-way or normal/repeated measured were used based on the variables)
697 was used. The asterisks in the figures represent the p values of post-hoc tests corresponding to the
698 following values *$p < 0.05$, **$p < 0.01$, ***$p < 0.001$, ****$p < 0.0001$. Following histology and imaging,
699 any mouse whose targeted injection site was missed or overly expressed was excluded from
700 experimental analysis.

701

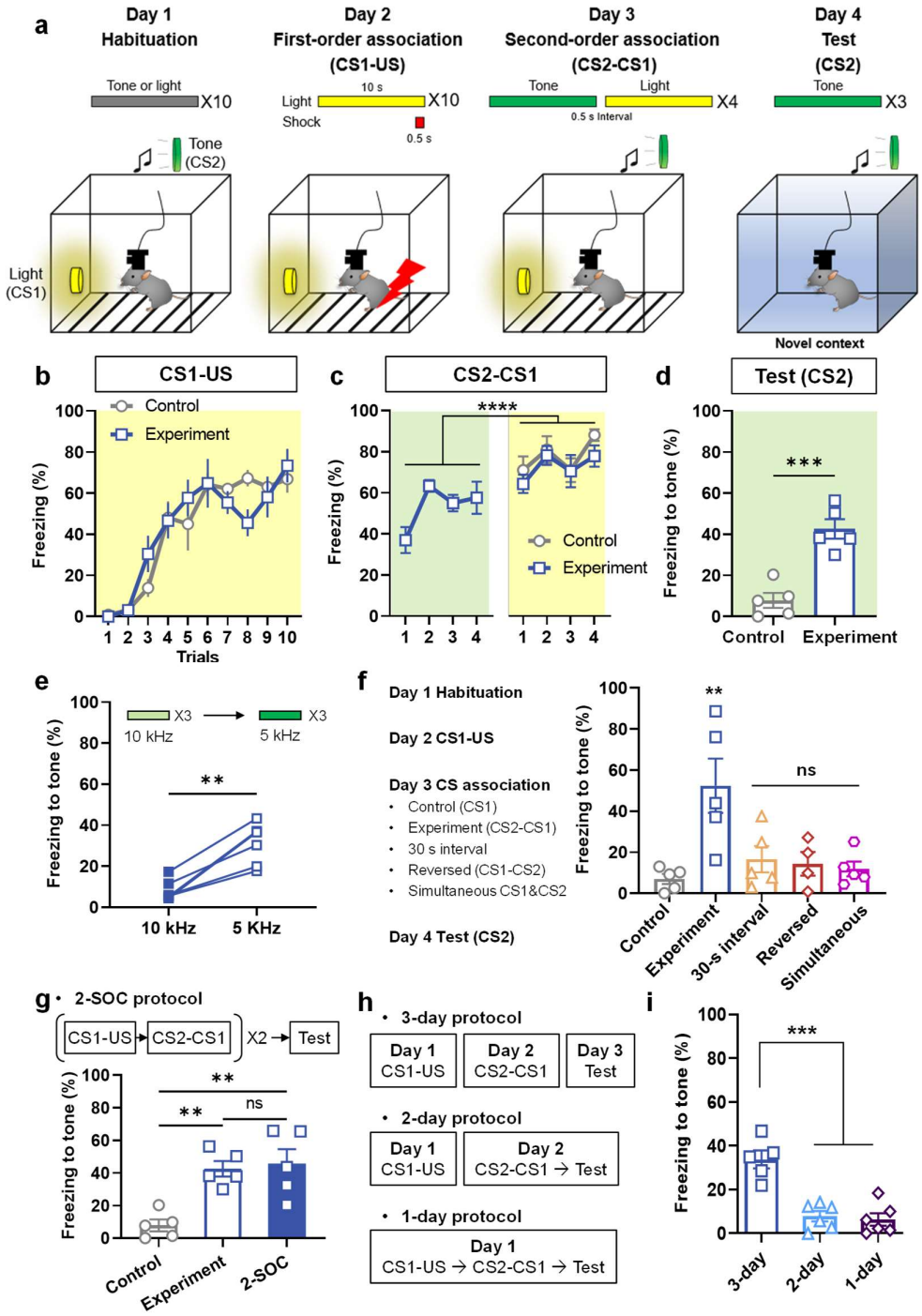

Figure 1: Validation of second-order fear conditioning (SOC) paradigm and behavioral responses in mice. a, Schematic representation of the standard SOC paradigm. **b**, Acquisition of first-order fear conditioning measured by freezing behavior to a light CS1 across trials for both control and experimental groups ($n = 5$ for both group). **c**, Freezing behavior during the CS2-CS1 association phase. Note that the control group was not exposed to tone CS2 in this session ($n = 5$ for both groups). **d**, Average freezing level across 3 trials of tone exposure on the test day ($n = 5$ for both groups). **e**, Freezing

levels in response to 10 kHz and 5 kHz tones on the test day (n = 5). Note that 5 kHz tone was paired with light CS1, whereas 10 kHz tone was not. **f**, Experimental procedure for variable CS2-CS1 associations (Left). Freezing responses to tone CS2 on the test phase for the control, experimental group, and the three timing variants (Right, n = 5 for control, experiment, 30-s interval and simultaneous groups and n = 4 for reversed group). **g**, Comparison of freezing behavior with one or two training sessions; data from panel **d** are included for easier comparison (n = 5 for each group). **h**, Schematic depiction of SOC protocols with varying training durations. **i**, Freezing responses to tone CS2 on the test day across different SOC groups with varied training durations (n = 5 for 3-day group, and n = 6 for 2-day and 1-day groups). Data are presented as mean ± SEM, **$p < 0.01$, ***$p < 0.001$, ***$p < 0.0001$.

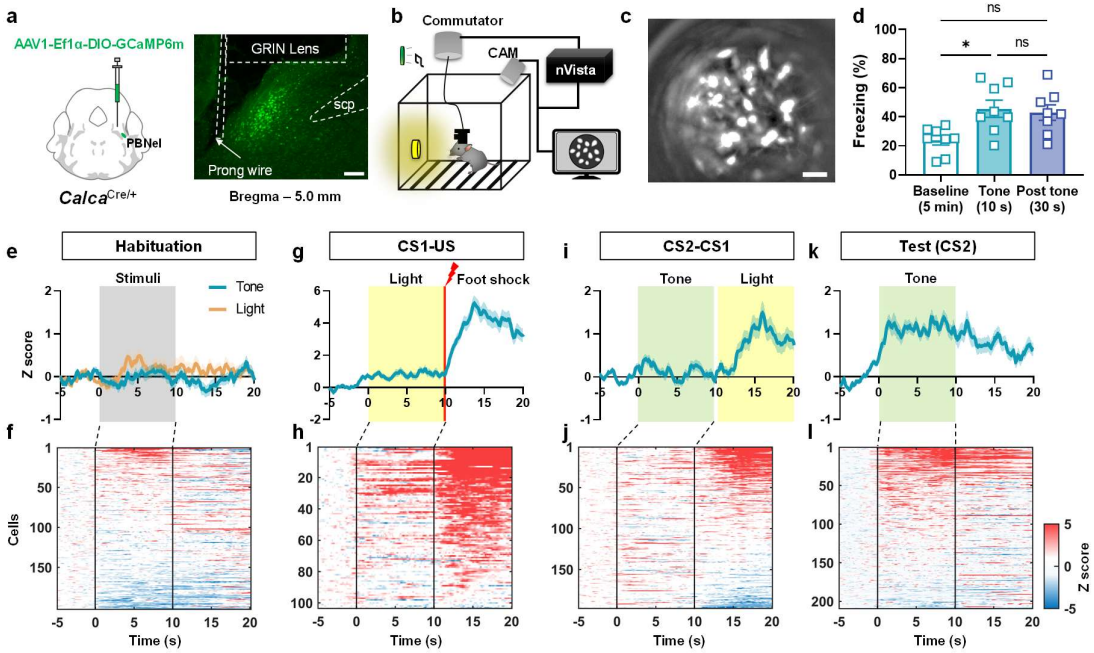

Figure 2: CGRP^{PBN} neuronal activity during second-order conditioning (SOC). a, Schematic illustration AAV-DIO-GCaMP6m viral injection into PBN and a representative image of the GRIN lens and stabilizing prong implanted in the PBN. Scale bar, 100 µm. **b**, Schematic illustration of the experimental setup for Ca^{2+} imaging in freely behaving mice. **c**, Representative field of view through the GRIN lens displays CGRP^{PBN} neurons expressing GCaMP6m. Scale bar, 50 µm. **d**, Freezing responses of animals subjected to Ca^{2+} imaging to the tone CS2 after SOC on test day. **e**, Average fluorescence activity of all neurons during habituation in response to light CS1 and tone CS2 (199 neurons). **f**, Individual neuronal responses to tone CS2 that are aligned by AUC during CS2. **g**, Average traces of all neurons during CS1-US pairing (103 neurons). **h**, Individual neuronal activity aligned by AUC after foot shock US. **i**, Average fluorescence activity of all neurons during CS2-CS1 pairing (199 neurons). **j**, Individual neuronal responses aligned by AUC of light CS1. **k**, Average traces of all CGRP^{PBN} neurons during test. **l**, Individual neuronal activity aligned by AUC during tone CS2 (209 neurons). Neuronal activity traces are average of trials. Data are mean ± SEM, *$p < 0.05$.

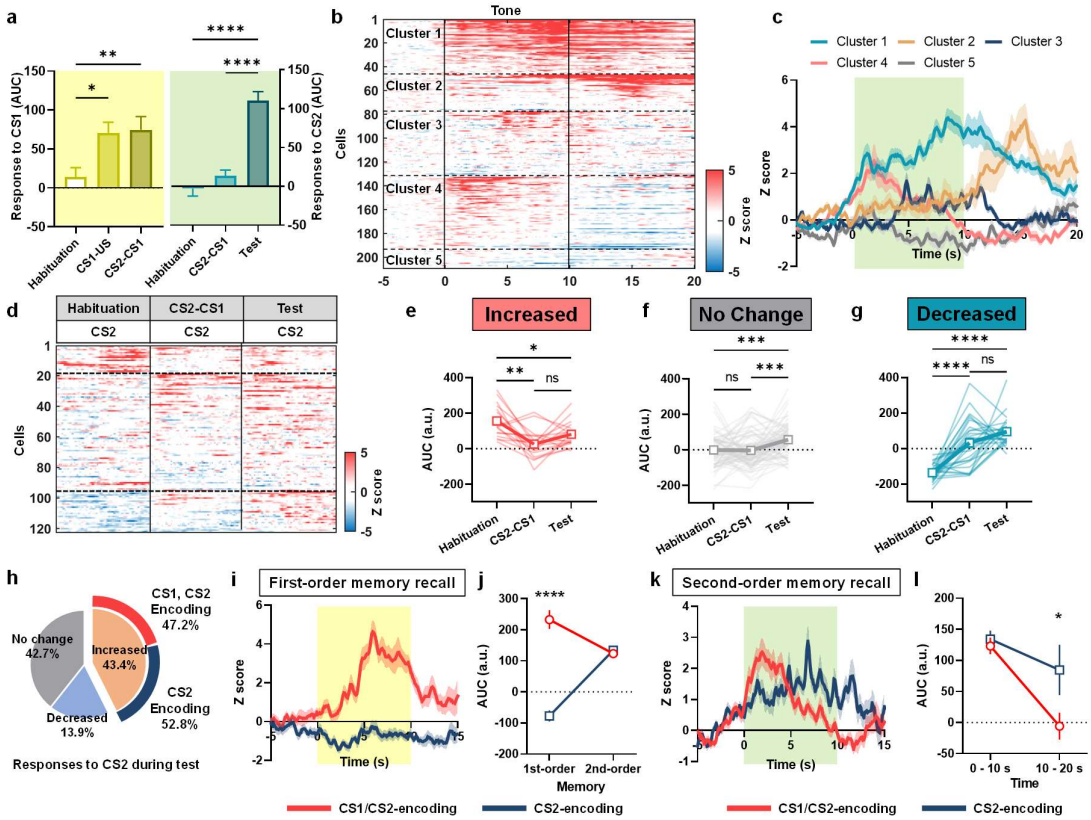

Figure 3: Heterogeneity of CGRP^{PBN} neuronal responses to conditioned tone (CS2) after second-order conditioning. a, Average AUC of CGRP^{PBN} neuronal activities in response to light CS1 (left) and tone CS2 (right) during SOC. The number of neurons in each day is 199 (habituation), 103 (CS1-US), 199 (CS2-CS1), and 209 (test). **b**, Heatmap of clustered individual neuronal response to tone CS2 in the test phase (n = 209 from 8 mice). **c**, K-means clustering of CGRP^{PBN} neurons based on their activity patterns during tone CS2 presentation on the test phase. **d**, Top, table showing experimental day and response information of heatmap. Bottom, heatmap of 122 neurons analyzed by longitudinal tracking of individual neuron activities to tone CS2 across experimental phases. Horizontal lines indicate classified neurons based on tone CS2 responses during habituation (top, increased; middle, no change; bottom, decreased). **e**, The average changes of area under the curve (AUC) over learning phases for neurons initially classified as "increased" response group during habituation. **f**, The average changes of AUC over phases for "no change" group during habituation. **g**, The average changes of AUC over phases for "decreased" group during habituation. **h**, Pie chart illustrating the proportion of neurons during tone CS2 in test phase (left) and proportion of CS2 responsive neurons based on activity to light CS1. **i**, Average traces of CS1/CS2 and CS2-encoding neurons during first-order memory recall (CS2-CS1 association). **j**, AUC of traces during first and second-order memory recall. **k**, Average traces of CS1/CS2-encoding neurons and CS2-encoding neurons during second-order memory recall (test). **l**, AUC of traces during CS2 (0 - 10 s) and post CS2 (10 - 20 s). Traces are average of trials. Data are mean ± SEM, *p < 0.05, **p < 0.01, ***p < 0.001, ****p < 0.0001.

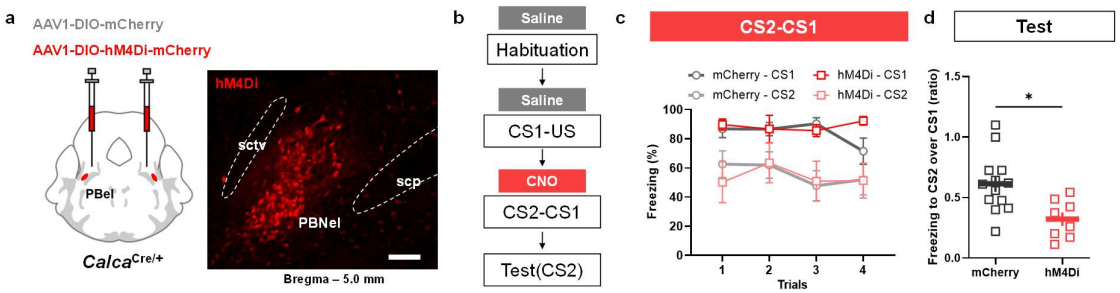

Figure 4: Chemogenetic inhibition of CGRP^{PBN} neurons during second-order association attenuates second-order memory. a, Schematic diagram representing bilateral injection of AAV-DIO-hM4Di-mCherry (hM4Di) or AAV-DIO-mCherry (control) into PBN and representative image of viral expression in PBN. Scale bar, 100 µm. **b**, Timeline summarizing experimental phases. **c**, Comparison of freezing behavior during light CS1 and tone CS2 presentation in the CS2-CS1 pairing phase for hM4Di and control groups. CNO was injected 30 min prior to session (n = 13 for mCherry and n = 8 for hM4Di). **d**, Second-order memory calculated as a ratio of freezing in response to tone CS2 (test) over freezing to CS1 (n = 13 for mCherry and n = 8 for hM4Di). Data are mean ± SEM, *p < 0.05.

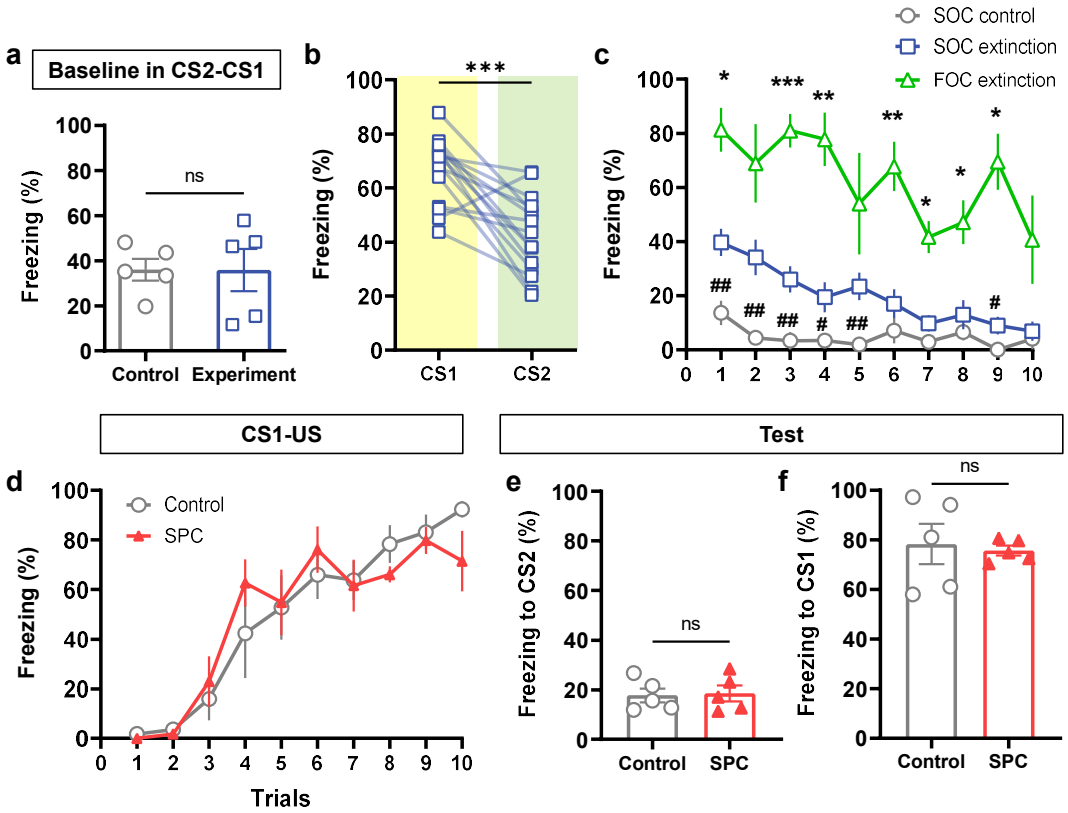

Extended Data Fig. 1: Extinction of SOC and sensory preconditioning in mice.

a, Freezing during baseline (1-min before session start) in CS2-CS1 association (n = 5 for each group). **b**, Comparison freezing to light CS1 during CS2-CS1 phase and freezing to tone CS2 during test phase (n = 15 for experimental animals in Fig. 1). **c**, Freezing level during extinction trials of first-order conditioning (FOC extinction, n = 4), second-order conditioning (SOC extinction, n = 11), and control (SOC control, n = 5). Asterisks (*) indicate comparison between FOC extinction and SOC extinction. Pound signs (#) indicate comparison between SOC extinction and control. **d**, Learning curves during CS1-US association of sensory preconditioning (n = 5 for control and 5 for sensory preconditioning group). SPC, sensory preconditioning. **e**, Freezing responses to the tone CS2 on test phase of sensory preconditioning protocol. **f**, Freezing responses to the light CS1 on test day. Data are mean ± SEM, *p < 0.05, **p < 0.01, ***p < 0.001, #p < 0.05, ##p < 0.01.

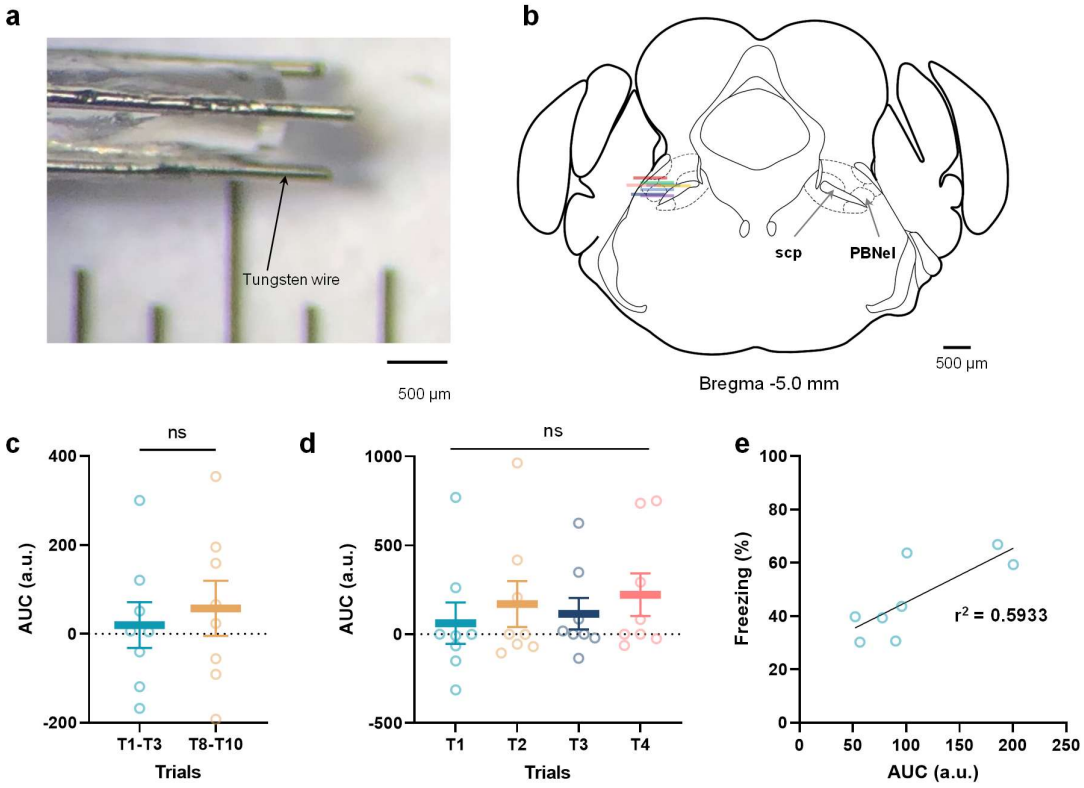

Extended Data Fig. 2: GRIN lens implantation in PBN and AUC analysis based on trials.

a, Picture of prong wires attached to GRIN lens for minimizing motion artifact. **b**, Schematic depiction of GRIN lens placements over PBN. Note that PBN section is adapted from Franklin and Paxinos mouse brain atlas[72]. **c**, AUC of $CGRP^{PBN}$ neurons during CS1 across the trials on the CS1-US association. **d**, AUC of $CGRP^{PBN}$ neurons during tone CS2 across the trials in CS2-CS1 association. **e**, Linear regression between AUC during tone CS2 in test day and freezing behavior. The equation of line graph is as $Y = 0.2018X + 25.04$. The data indicate individual animals; plotted as mean ± SEM.

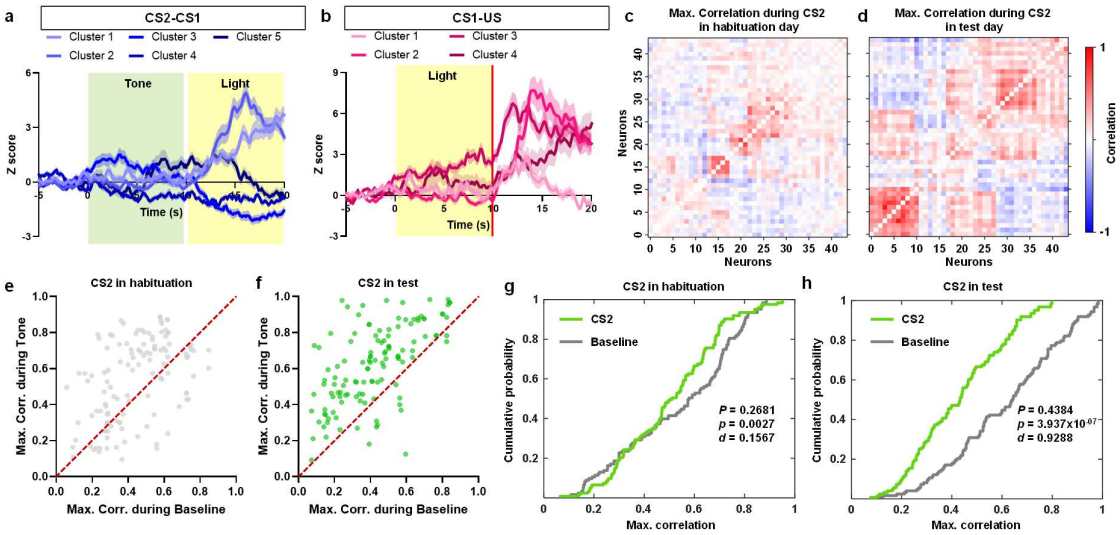

Extended Data Fig. 3: Cluster and correlation analysis of CGRP^{PBN} neurons during SOC.

a, Clustered activities of CGRP^{PBN} neurons during CS2-CS1 association. **b**, Clustered activities of CGRP^{PBN} neurons during CS1-US association. **c**, Heatmap of maximum correlations within CGRP^{PBN} neurons from representative animal before SOC (habituation). **d**, Heatmap of maximum correlations within CGRP^{PBN} neurons from representative animal after SOC (test). **e**, Linear regression of maximum correlations of CGRP^{PBN} neurons in habituation phase. **f**, Linear regression of maximum correlations of CGRP^{PBN} neurons in test day**.** **g**, Cumulative distribution function of maximum correlations during tone CS2 and baseline in habituation day. Note that baseline indicates neural activities of first 5 min in test chamber before session start. P indicates pairwise Pearson's correlation. *p* indicates paired t-test. *d* indicates Cohen's *d* which represents effect size. **h**, Cumulative distribution function of mean correlations during tone CS2 and baseline in test day. Data are mean ± SEM.

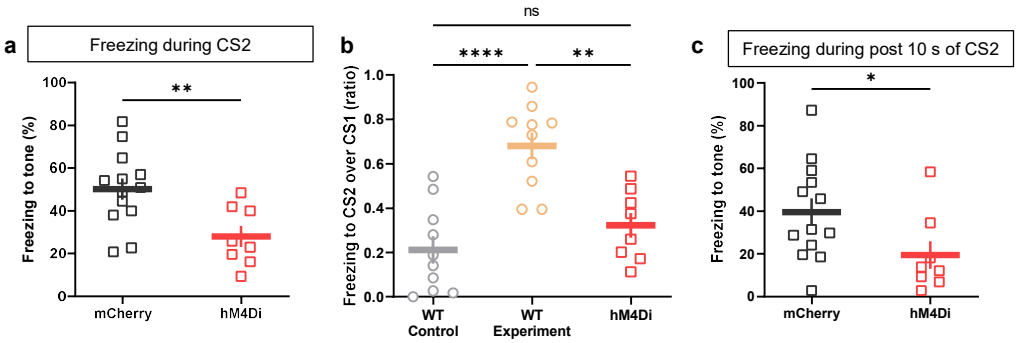

Extended Data Fig. 4: Transient inhibition of CGRP^{PBN} neurons during second-order association attenuates freezing to CS2 and post CS2. a, Freezing responses to tone CS2 of control and hM4Di groups after SOC. **b**, Comparison of freezing ratio CS2 over CS1 between WT mice experiments and hM4Di group. Note that WT control did not receive second-order association. **c**, Freezing responses to post CS2 (10 sec after CS2) of control and hM4Di groups in test day. Data are trial average of each mouse; plotted as mean ± SEM, *$p < 0.05$, **$p < 0.01$, ****$p < 0.0001$.

805 **Summary of the statistical analysis**

Figure	Mean (number of data)	Normality test (Shapiro-Wilk test, P>0.05; passed)	Statistical test	Comparison	Results (P value)
Fig. 1c	Experiment CS1 = 72.71 (5) Experiment CS2 = 53.23 (5) Control CS1 = 77.77 (5)	Experiment CS1, P = 0.3296 Experiment CS2, P = 0.3635 Control CS1, P = 0.2670	Two-way RM ANOVA F (1, 8) = 86.61	Experiment CS1 vs. Experiment CS2	< 0.0001
			Two-way ANOVA F (1, 8) = 43.17	Control CS1 vs. Experiment CS2	0.0002
Fig. 1d	Control = 7.844 (5) Experiment = 42.53 (5)	P = 0.5247 for control P = 0.6564 for Experiment	Unpaired t-test (Two-tailed) t = 5.826, df = 8	Control vs. Experiment	0.0004
Fig. 1e	Mean difference = 22.52 (5)	10 kHz, P = 0.0486 5 kHz, P = 0.4834	Paired t-test (Two-tailed) t = 6.260, df = 5	10 kHz vs 5 kHz	0.0015
Fig. 1f	Control = 7.010 (5) Experiment = 52.39 (5) 30-s interval = 11.84 (5) Reversed = 16.60 (4) Simultaneous = 14.36 (5)	Control, P = 0.9188 Experiment, P = 0.9488 30-s interval, P = 0.2929 Reversed, P = 0.4087 Simultaneous, P = 0.9273	One-way ANOVA F (4, 19) = 6.18 P = 0.0023	Experiment vs. Control	0.0012
				Experiment vs. 30-s interval	0.0033
				Experiment vs. Reversed	0.0091
				Experiment vs. Simultaneous	0.0090
Fig. 1i	3-day = 33.78 (5) 2-day = 7.852 (6) 1-day = 6.370 (6)	3-day, P = 0.9668 2-day, P = 0.4096 1-day, P = 0.2913	One-way ANOVA F (2, 14) = 23.39 P < 0.0001	3-day vs. 2-day	< 0.0001
				2-day vs. 1-day	< 0.0001
Fig. 2d	Baseline = 23.76 (8) Tone = 45.49 (8) Post tone = 42.86 (8)	Baseline, P = 0.1290 Tone, P = 0.6057 Post tone, P = 0.9724	One-way RM ANOVA F (1.810, 12.67) = 7.242 P = 0.0092	Baseline vs. Tone	0.0464
				Baseline vs. Post tone	0.0663
				Tone vs Post tone	0.9473
Fig. 3a (left)	Habituation = 13.81 (199) CS1-US = 74.59 (103) CS2-CS1 = 74.59 (199)	Habituation, P < 0.0001 CS1-US, P = 0.0016 CS2-CS1, P < 0.0001	One-way ANOVA F (2, 496) = 5.493 P = 0.0044	Habituation vs. CS1-US	0.0470
				Habituation vs. CS2-CS1	0.0061
				CS1-US vs. CS2-CS1	0.9971
Fig. 3a (right)	Habituation = -3.068 (199) CS2-CS1 = 13.17 (199) Test = 110.2 (209)	Habituation, P < 0.0001 CS1-CS2, P = 0.0045 Test, P < 0.0001	One-way ANOVA F (2, 604) = 38.93 P < 0.0001	Habituation vs. CS2-CS1	0.4825
				Habituation vs. Test	< 0.0001
				CS2-CS1 vs. Test	< 0.0001
Fig. 3e	Habituation = 155.5 (18) CS2-CS1 = 25.39 (18) Test = 81.08 (18)	Habituation, P = 0.2309 CS2-CS1, P = 0.4220 Test, P = 0.1555	One-way RM ANOVA F (1.833, 31.15) = 12.15 P = 0.0002	Habituation vs. CS2-CS	0.0013
				Habituation vs. Test	0.0232
				CS2-CS1vs. Test	0.0749
Fig. 3f	Habituation = -2.388 (76) CS2-CS1 = -4.382 (76)	Habituation, P = 0.0593 CS2-CS1, P = 0.0086	One-way RM ANOVA	Habituation vs. CS2-CS1	0.9911

	Test = 55.77 (76)	Test, P = 0.0734	F (1.972, 147.9) = 10.45 P<0.0001	Habituation vs. Test	0.0003
				CS2-CS1 vs. Test	0.0005
Fig. 3g	Habituation = -135.4 (28) CS2-CS1 = 32.57 (28) Test = 95.70 (28)	Habituation, P = 0.9992 CS2-CS1, P = 0.3078 Test, P = 0.0027	One-way RM ANOVA F (1.440, 38.88) = 38.72 P<0.0001	Habituation vs. CS2-CS1	<0.0001
				Habituation vs. Test	<0.0001
				CS2-CS1 vs. Test	0.1586
Fig. 3j	Mean difference = 309.9 in 1st-order -10.86 in 2nd-order CS1/CS2 (25) CS2 (28)	CS1/CS2, P = 0.0730 CS2, P = 0.4432	Two-way RM ANOVA F (1, 51) = 72.80 P<0.0001	CS1/CS2 vs. CS2 in 1st-order	<0.0001
				CS1/CS2 vs. CS2 in 2nd-order	0.9087
Fig. 3i	Mean difference = -10.86 in 0-10 s -90.49 in 10-20 s CS1/CS2 (25) CS2 (28)	CS1/CS2, P = 0.2738 CS2, P < 0.0001	Two-way RM ANOVA F (1, 51) = 4.049 P=0.0495	CS1/CS2 vs. CS2 in 0-10 s	0.9451
				CS1/CS2 vs. CS2 10-20 s	0.0286
Fig. 4c	mCherry light = 83.88 (13) hM4Di light = 88.64 (8) mCherry tone = 56.13 (13) hM4Di tone = 54.02 (8)	mCherry light, P = 0.5215 hM4Di light, P = 0.7614 mCherry tone, P = 0.3436 hM4Di tone, P = 0.4700	Two-way ANOVA F (3,57) = 1.757 P = 0.1656	mCherry light vs. hM4Di light	0.3958
			Two-way ANOVA F (3, 57) = 0.2211 P = 0.8813	mCherry tone vs. hM4Di tone	0.68347
Fig. 4d	mCherry = 0.6133 (13) hM4Di = 0.3221 (8)	mCherry, P = 0.5845 hM4Di, P = 0.6684	Unpaired t-test (Two-tailed) t = 3.038, df = 19	mCherry vs. hM4Di	0.0068
Extended Data Fig. 1a	Control = 36.00 (5) Experiment = 35.89 (5)	Control, P = 0.7714 Experiment, P = 0.2014	Unpaired t-test (Two-tailed) t = 0.0100, df = 8	Control vs. Experiment	0.9922
Extended Data Fig. 1b	Mean difference = -24.03 (15)	CS1, P = 0.2244 CS2, P = 0.6454	Paired t-test (Two-tailed) t = 4.897, df = 14	CS1 vs CS2	0.0002
Extended Data Fig. 1c	SOC control = 13.67, 4.40, 3.33, 3,40, 1,93, 7.07, 2,93, 6,53, 0.00, 4.07 (5) SOC extinction = 39.70, 34.12, 26.03, 19.45, 23.42, 17.03, 9.79, 12,97, 9.03, 6,88 (11) FOC extinction = 81.33, 68,92, 81,00, 77,83, 54,00, 67,57, 41,67, 47.08, 69.60, 40.67 (4)	SOC control, P = 0.0905 SOC extinction, P = 0.5067 FOC extinction, P = 0.1502	Two-way RM ANOVA F (18, 153) = 1,760 P = 0.0350	SOC control vs. SOC extinction	0.0057, 0.0027, 0.0043, 0.0480, 0.0048, 0.3734, 0.1322, 0.5704, 0.0486, 0.8603
				SOC extinction vs. FOC extinction	0.0020, 0.0407, 0.0004, 0.0080, 0.1331, 0.0060, 0.0126, 0.0224,

					0.0138, 0.2085
Extended Data Fig. 1d	Control = 50.00 (5) SPC = 49.73 (5)	Control, P = 0.3065 SPC, P = 0.0289	Two-way RM ANOVA F (9, 72) = 1.033 P = 0.4230	Control vs. SPC	0.9697
Extended Data Fig. 1e	Control = 17.71 (5) SPC = 18.56 (5)	Control, P = 0.4262 SPC, P = 0.6146	Unpaired t-test (Two-tailed) t = 0.1974, df = 8	Control vs. SPC	0.8485
Extended Data Fig. 1e	Control = 78.29 (5) SPC = 75.62 (5)	Control, P = 0.2897 SPC, P = 0.4856	Unpaired t-test (Two-tailed) t = 0.3184, df = 8	Control vs. SPC	0.7584
Extended Data Fig. 2c	Trial 1-3 = 21.50 (8) Trial 8-10 = 79.32 (8)	Trial 1-3, P = 0.6997 Trial 4-6, P = 0.9854	Paired t-test (Two-tailed) t = 0.0869, df = 7	Trial 1-3 vs. Trial 8-10	0.4135
Extended Data Fig. 2d	T1 = 61.75 (8) T2 = 169.6 (8) T3 = 115.0 (8) T4 = 221.8 (8)	T1, P = 0.0788 T2, P = 0.0128 T3, P = 0.0388 T4, P = 0.0134	One-way RM ANOVA F (1.775, 12.42) = 0.4567 P = 0.6211	T1vs. T2	0.9216
				T1 vs. T3	0.9828
				T1 vs. T4	0.8374
				T2 vs. T3	0.9798
				T2 vs. T4	0.9070
				T3 vs. T4	0.7088
Extended Data Fig. 2e	AUC = 107.34 (8) Freezing = 45.49 (8)	AUC, P = 0.2037 Freezing, P = 0.0678	Simple linear regression F (1, 6) = 8.751 P = 0.0253	Equation Y = 0.2018X + 25.04	r^2 = 0.5933
Extended Data Fig. 3g	Baseline = 0.443 (122) CS2 = 0.540 (122)	Baseline, P = 0.0222 CS2, P < 0.0001	Pairwise Pearson's correlation P = 0.2681	Baseline vs. CS2	P = 0.0027 Cohen's d = 0.1567
Extended Data Fig. 3h	Baseline = 0.421 (122) CS2 = 0.618 (122)	Baseline, P = 0.0046 CS2, P = 0.0124	Pairwise Pearson's correlation P = 0.4384	Baseline vs. CS2	P = $3.937*10^{-7}$ Cohen's d = 0.9288
Extended Data Fig. 4a	mCherry = 50.24 (13) hM4Di = 28.03 (8)	mCherry, P = 0.9041 hM4Di, P = 0.6037	Unpaired t-test (Two-tailed) t = 3.001, df = 19	mCherry vs. hM4Di	0.0073
Extended Data Fig. 4b	WT control = 0.2114 (10) WT experiment = 0.6799 (10) hM4Di = 0.3221 (8)	WT control, P = 0.0.2596 WT experiment, P = 0.3165 hM4Di = 0.6684	One-way ANOVA F (2, 25) = 17.48 P < 0.0001	hM4Di vs. WT control	0.4269
				hM4Di vs. WT experiment	0.0011
				WT control vs. WT experiment	<0.0001
Extended Data Fig. 4c	mCherry = 39.54 (13) hM4Di = 19.43(8)	mCherry, P = 0.8760 hM4Di, P = 0.0439	Unpaired t-test (Two-tailed) t = 2.095, df = 19	mCherry vs hM4Di	0.0498

806